Journal Homepage: - www.journalijar.com
INTERNATIONAL JOURNAL OF ADVANCED RESEARCH (IJAR)
Article DOI: 10.21474/IJAR01/1543
DOI URL: http://dx.doi.org/10.21474/IJAR01/1543
ISSN NO. 2320-5407

RESEARCH ARTICLE

EFFECT OF ZINC SUBSTITUTION ON STRUCTURAL AND IMPEDANCE PROPERTIES OF LAYERED $LiNi_{1/3}Co_{(1/3-x)}Mn_{1/3}Zn_xO_2$ ($0.05 \leq x \leq 0.2$) CATHODE MATERIALS

G.Tewodros Aregai, K. Vijaya Babu, B. Vikram Babu, P.S.V. Subba Rao and V.Veeraiah.

Manuscript Info

Manuscript History

Received: 15 July 2016
Final Accepted: 30 August 2016
Published: September 2016

Key words:-
Layered Structure, Lithium Nickel Manganese Cobalt Oxides, XRD, LCR

Abstract

The aim of this paper is to study the effect of Zn substituted in place of Co in $LiNi_{1/3}Co_{1/3}Mn_{1/3}O_2$ synthesized by solid state reaction method. A series of materials based on the $LiNi_{1/3}Co_{(1/3-X)}Mn_{1/3}Zn_XO_2$ ($0.05 \leq x \leq 0.2$) system were prepared by solid state reaction method and their phase formation processes, crystal structures, impedance and dielectric were studied by XRD and LCR meter. The X-ray diffraction (XRD) reviles the layered structure of the hexagonal α-$NaFeO_2$ structure with a space group of $R\bar{3}m$. The presence of grain (bulk) effect in the compound was observed. The frequency-dependent electrical data were used to study the conductivity mechanism. An analysis of the electric impedance with frequency at different temperatures has provided some information to support suggested conduction mechanism.

Introduction:-

The development of lithium ion batteries is important to improve the energy and power efficiency of such devices, cost effective and their impact on the environment. Research to develop positive materials for such applications is of major importance. Mixing proper levels of these three transition metals to get the advantageous qualities of each led to the discovery of this material. This material is derived from $LiNi_{1-y-z}Mn_yCo_zO_2$ family group (where y = z = 1/3) which were first published in 1999 by Liu et al [1] and in 2000 by Yoshio et al [2]. Yoshio hypothesized that the addition of cobalt to $LiMn_{1-y}Ni_yO_2$ would stabilize the structure in a strictly two-dimensional way by jamming the nickel atoms from inflowing the lithium layer while Mn and Ni content would grant increased structural stability and high capacities respectively. Mixing these three cations at finest levels is very important since too much of Co would lead to decrease in capacity, too much of Ni will result in cation mixing and too much of Mn can lead to structural change. Since the layered transition metal oxide $LiNi_{1/3}Co_{1/3}Mn_{1/3}O_2$ was initially proposed by Ohzuku and Makimura [3] in 2001, it has been extensively studied[4-6] due to its higher reversible capacity, lower cost, less toxicity, and enhanced safety features compared to conventional $LiCoO_2$. The $LiNi_{1/3}Co_{1/3}Mn_{1/3}O_2$ powder has a typical hexagonal α-$NaFeO_2$ structure with a space group of $R\bar{3}m$. The $LiNi_{1/3}Co_{1/3}Mn_{1/3}O_2$ cathode material can deliver a high capacity of ca 200 $mAh \cdot g^{-1}$ when it is charged to 4.6 V (*vs* Li/ Li^+) [7-11]. It is considered to be one of the best candidate cathode materials for high-power applications [12]. On the other hand, there are still two important problems limiting the applications of $LiNi_{1/3}Co_{1/3}Mn_{1/3}O_2$ cathode material in high power lithium ion batteries. One is the serious capacity fading, especially if cycled at 4.6 V (*vs* Li/Li^+) [7, 8] and its poor rate capacity due to its low Li ion diffusion as well as the electronic conductivity. To overcome both problems of $LiNi_{1/3}Co_{1/3}Mn_{1/3}O_2$ cathode material, one significant approach is doping by transition or non-transition metals such as Ti, Cr, La, Cu, Al, Zn and Mg [13-15]. Partial substitution Zn in place of Co has been proved an effective method

Corresponding Author:- G.Tewodros Aregai.

in modifying the electronic structure and improving the electrochemical performances as well as to minimize the cost and environment issues associated with cobalt. In this work, we are reporting partial substitution of Zn on the $LiNi_{1/3}Co_{(1/3-x)}Mn_{1/3}Zn_xO_2$ ($0.05 \leq x \leq 0.2$) cathode materials synthesized by high temperature solid-state reaction method and the effects on structure, morphology, electrical and dielectric properties were investigated in detail in order to overcome the above mentioned problems.

Preparation and experimental techniques:-

The cathode compositions are synthesized by high temperature solid-state reaction method from stoichiometric amounts of Li_2CO_3 (Himedia 99.9%), NiO (Himedia 99.9%), Co_2O_3 (Himedia 99.9%), MnO_2 (Himedia 99.9%) and ZnO (Himedia 99.9%).

$0.5Li_{2C}O_{3\,3}+1/3NiO+0.1417Co_2O_3+0.05ZnO+1/3MnO_2 \rightarrow LiNi_{1/3}Co_{0.28333}Zn_{0.05}Mn_{1/3}O_2 + gas \uparrow$

$0.5Li_{2C}O_3+1/3NiO + 0.117Co_2O_3+_0.1ZnO +1/3MnO_2 \rightarrow LiNi_{1/3}Co_{0.23333}Zn_{0.1M}n_{1/3}O_{\,2} + gas \uparrow$

$0.5Li_2CO_3 +1/3NiO+0.0917Co_2O_3+0.15ZnO +1/3MnO_2 \rightarrow LiNi_{1/3}Co_{0.18333}Zn_{0.15}Mn_{1/3}O_2 + gas \uparrow$

$0.5Li_2CO_3 +1/3NiO+ 0.067Co_2O_3 + 0.2ZnO +1/3MnO_2 \rightarrow LiNi_{1/3}Co_{0.13333}Zn_{0.2}Mn_{1/3}O_2 + gas \uparrow$

A slight excess amount of lithium (5%) was used to compensate for any loss of the metal which might have occurred during the calcination at high temperature. The solid state reaction synthesis method involves three steps. First, the precursors, as raw materials, are well mixed and thoroughly ground with agate mortar, then subjected to heat treatment at a temperature of 500ºC for 5 hours and 800ºC for 10 hours to dry the samples free from gases and impurities. Then, this powder was cooled at the rate of 5 ºC/ min. Finally, the mixture is reground and sintered at temperatures 900 °C for 18 hours to complete the chemical reaction in air using a muffle box furnace. For electrical study, pellets with diameter around 11-13 mm in diameter and 1.1 to 1.3 mm in thickness are used.

The powder X-ray diffraction (XRD) data of the sample is collected on a PANalytical X-pert pro diffractometer with diffraction angles of 10º and 90º in increments of 0.02º. The unit cell lattice parameter is obtained by the unit cell software from the 2θ and (h k l) values. Further, the crystallite size of the sample is obtained by applying the Scherrer's equation from XRD pattern. The electrical measurements are performed using a Phase Sensitive Multimeter (Model: PSM 1700, UK) over the frequency range from 1 Hz to 1 MHz from room temperature to 393.15 K.

Results and Discussion:-

XRD Studies:-

Figure 1 shows the XRD patterns of $LiNi_{1/3}Co_{(1/3-X)}Mn_{1/3}Zn_XO_2$ (x=0, 0.05, 0.1, 0.15, and 0.2) cathode materials. All the $LiNi_{1/3}Co_{(1/3-X)}Mn_{1/3}Zn_XO_2$ (x=0, 0.05, 0.1, 0.15, and 0.2) cathode material samples have a typical hexagonal α-$NaFeO_2$ structure (JCPDS card number 50-0653); almost no diffraction peaks of impurity can be found for $LiNi_{1/3}Co_{(1/3-X)}Mn_{1/3}Zn_XO_2$ (x=0, 0.05, 0.1, 0.15 and 0.2) revealing that partial substitution of Zn in the $LiNi_{1/3}Co_{1/3}Mn_{1/3}O_2$ cannot change the crystal structure. This result could indicate that the Zn element is totally inserted into the lattice of $LiNi_{1/3}Co_{1/3}Mn_{1/3}O_2$. Moreover, the diffraction patterns show clear splitting of the hexagonal characteristic doublets of (006)/(102) and (108)/(110); this can be ascribed to the layered structure of $LiNi_{1/3}Co_{1/3}Mn_{1/3}O_2$ [16]. Table 1 gives the refined lattice parameters of $LiNi_{1/3}Co_{(1/3-X)}Mn_{1/3}Zn_XO_2$ (x=0, 0.05, 0.1, 0.15 and 0.2). The lattice expansions are slightly increased with Zn-doped content, which further illustrates that the Zn^{2+} ions have doped into the lattice of $LiNi_{1/3}Co_{1/3}Mn_{1/3}O_2$ during the calcined process. Since the metal ions, for example, Ni^{2+} (0.069 nm), Co^{3+} (0.0545 nm), and Mn^{4+} (0.054 nm), have smaller ion radius than that of Zn^{2+}, when they are replaced by the Zn^{2+} (0.074 nm), Zn^{2+} ions would enlarge the lattice parameter. Besides, the values of $I_{(003)}/I_{(104)}$ are $\geq$1.2, indicating that the samples have low cation mixing [17].The cation mixing will lead to an incensement of disorder, making an undesirable electrochemical performance of $LiNi_{1/3}Co_{1/3}Mn_{1/3}O_2$, for example, low lithium conductivity, low capacity, and poor cyclic performance [18]. For layered compounds, a higher value of *c*/*a* is desirable for better hexagonal structure [19].

Crystallite sizes for $LiNi_{1/3}Co_{(1/3-X)}Mn_{1/3}Zn_XO_2$ (x=0, 0.05, 0.1, 0.15 and 0.2) cathode materials are calculated by the Scherrer's equation as:

$L = \frac{k\lambda}{\beta \cos\theta}$, where *k* is the shape factor of 0.9 for spherical crystals, λ is the X-ray wavelength, β is half maximum intensity broadening (FWHM) in radians corrected for the instruments standard line width, and θ is the Bragg angle. L is the calculated mean size of the crystalline domains, equal to the particle size of single crystallites. In order to evaluate the influence of the substituted Zn ions on the structural properties of $LiNi_{1/3}Co_{(1/3-X)}Mn_{1/3}Zn_XO_2$ (x=0, 0.05, 0.1, 0.15 and 0.2), we calculated the lattice parameters, the volume of the unit cells, R-factor and the crystallite sizes of all samples from the XRD patterns. The obtained results are summarized in Table 1.

Table 1:- Lattice constants, c/*a* value, cell volume and crystallite sizes of synthesized $LiNi_{1/3}Co_{(1/3-X)}Mn_{1/3}Zn_XO_2$ (x = 0.05, 0.1, 0.15 and 0.2) compounds

Compound	*a* (Å)	c (Å)	c/*a*	V $(Å)^3$	$I_{(003)}/I_{(104)}$ R-factor	Crystallite size (nm)
$LiNi_{1/3}Co_{0.28333}Zn_{0.05}Mn_{1/3}O_2$	2.867	14.208	4.96	101.13	1.48	6.09
$LiNi_{1/3}Co_{0.23333}Zn_{0.1}Mn_{1/3}O_2$	2.864	14.24	4.97	101.19	1.46	5.8
$LiNi_{1/3}Co_{0.18333}Zn_{0.15}Mn_{1/3}O_2$	2.860	14.32	5.00	101.49	1.45	6.01
$LiNi_{1/3}Co_{0.13333}Zn_{0.2}Mn_{1/3}O_2$	2.85	14.23	4.97	101.47	1.43	6.12

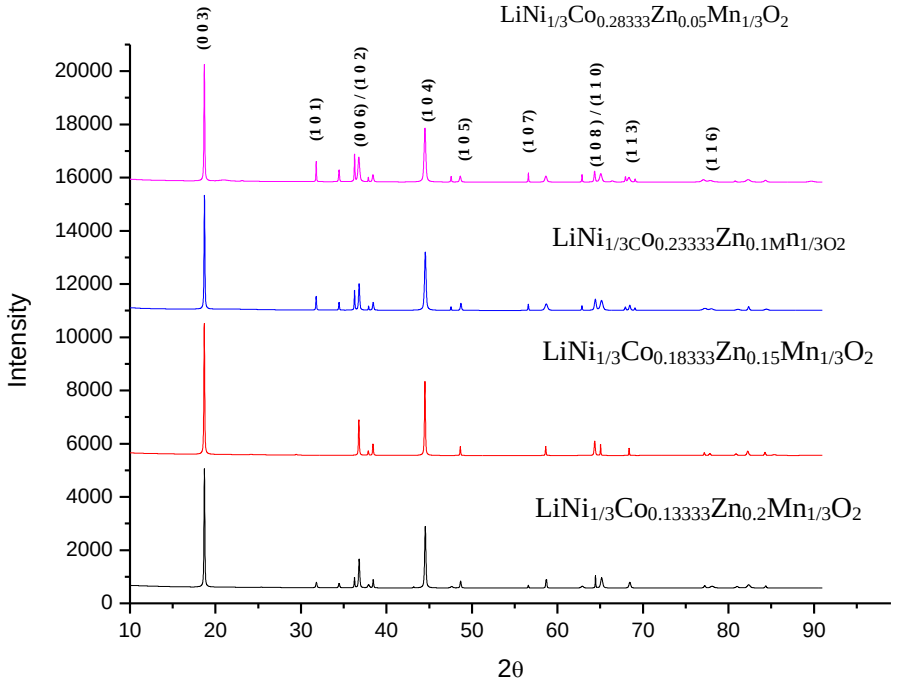

Figure 1:- XRD patterns for $LiNi_{1/3}Co_{0.28333}Zn_{0.05}Mn_{1/3}O_2$, $LiNi_{1/3}Co_{0.23333}Zn_{0.1}Mn_{1/3}O_2$, $LiNi_{1/3}Co_{0.18333}Zn_{0.15}Mn_{1/3}O_2$, and $LiNi_{1/3}Co_{0.13333}Zn_{0.2}Mn_{1/3}O_2$ samples

Impedance Analysis:-

This technique is useful to investigate the electrical conduction across intra-grain, grain boundary and electrode specimen interface. Moreover, the CIS measurement technique is also useful to investigate the temperature and frequency dependent behaviour of AC conductivity and dielectric constant. In general, electrochemical impedance studies are carried out to have better understanding of certain aspects of a lithium cell such as failure mechanism [20], self discharge [21], lithium cycling efficiency [22], interfacial phenomenon between electrode and electrolyte [23] and lithium cation diffusion in the electrode and the electrolyte [24].

Nyquist plots:-

The Cole-Cole plots of a series of $LiNi_{1/3}Co_{(1/3-X)}Mn_{1/3}Zn_XO_2$ (x= 0.05, 0.1and 0.15) powder materials measured at various temperatures are shown in Figure 2 (a) to (c). The plots clearly show that there is an inclined straight line at lower frequency region followed by a semi circular arc at the higher frequency region. The low frequency semicircle is due to the grain and the higher depicts the bulk (grain) effect. The obtained curves for each sample appeared in the form of single semicircles at various temperatures. No other curves are observed in the lower frequency regions. Therefore, the semicircles of each sample are attributed to bulk conductivity, suggesting that the conductivity is mixed electronic and ionic in character. The intersections of the semicircles at lower frequencies with the Z'-axis are taken as the sample grain or bulk resistance. It is observed that resistivity of the samples dramatically decreases with the increase in temperature. As a result the diameter of the semicircle decreases with increasing temperature. On the other hand, it is observed that all arcs in the impedance plots are not perfect semicircles, which means that the highest frequency arcs do not intersect with the Z' axis.

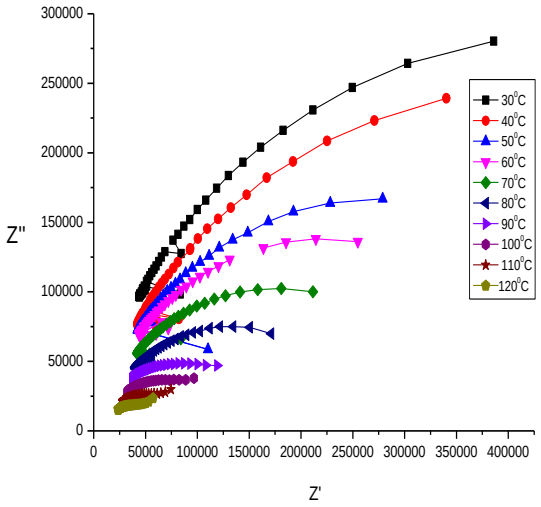

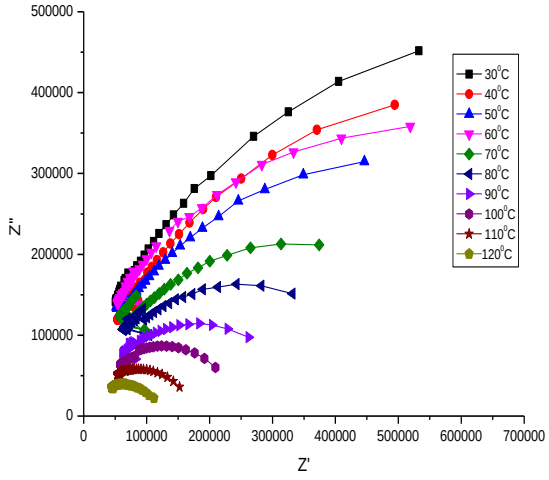

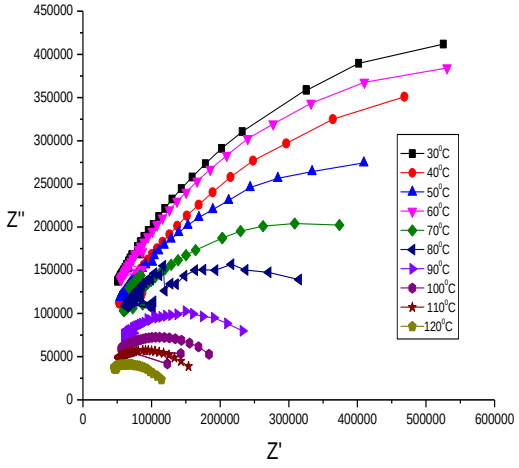

Figure 2:- (a-c) cole-cole plots for $LiNi_{1/3}Co_{0.28333}Zn_{0.05}Mn_{1/3}O_2$, $LiNi_{1/3}Co_{0.23333}Zn_{0.1}Mn_{1/3}O_2$ and $LiNi_{1/3}Co_{0.18333}Zn_{0.15}Mn_{1/3}O_2$

AC conductivity and Activation energy:-

A.C conductivity is one of the studies done on solids in order to characterize the bulk resistance of the crystalline sample. Measurement of A.C conductivity can be done by different techniques. In the present work the A.C conductivity is calculated from dielectric data using the relation:

$$\sigma_{ac} = \omega \varepsilon_r \varepsilon_0 \tan\delta \quad \text{Where } \omega = 2\pi f$$

The variation of A.C electrical conductivity for $LiNi_{1/3}Co_{(1/3-X)}Mn_{1/3}Zn_XO_2$ (x= 0.05, 0.1 and 0.15) as a function of frequency at different temperatures is shown in Figure 3(a-c). The conductivity spectrum displays characteristic conductivity dispersion throughout the frequency ranges b/n 50 Hz and 5.2 KHz. At high frequency independent plateau is observed, whereas in the low frequency region dispersion of conductivity is still retained. The crossover from the frequency independent region to the frequency dependent regions shows the onset of the conductivity relaxation, indicating the transition from long range hopping to the short range ionic motion. The frequency of onset of conductivity relaxation shifts with temperature to higher frequency side.

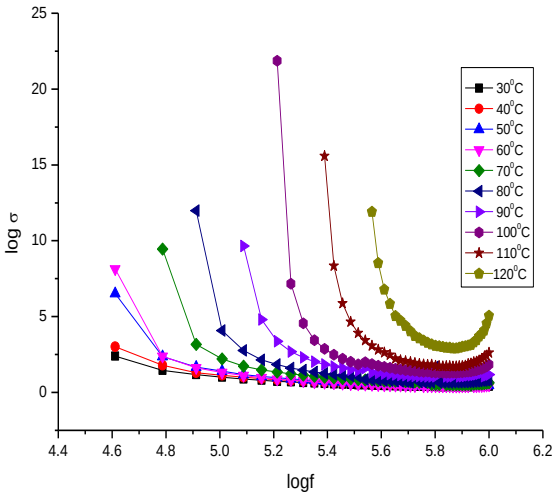

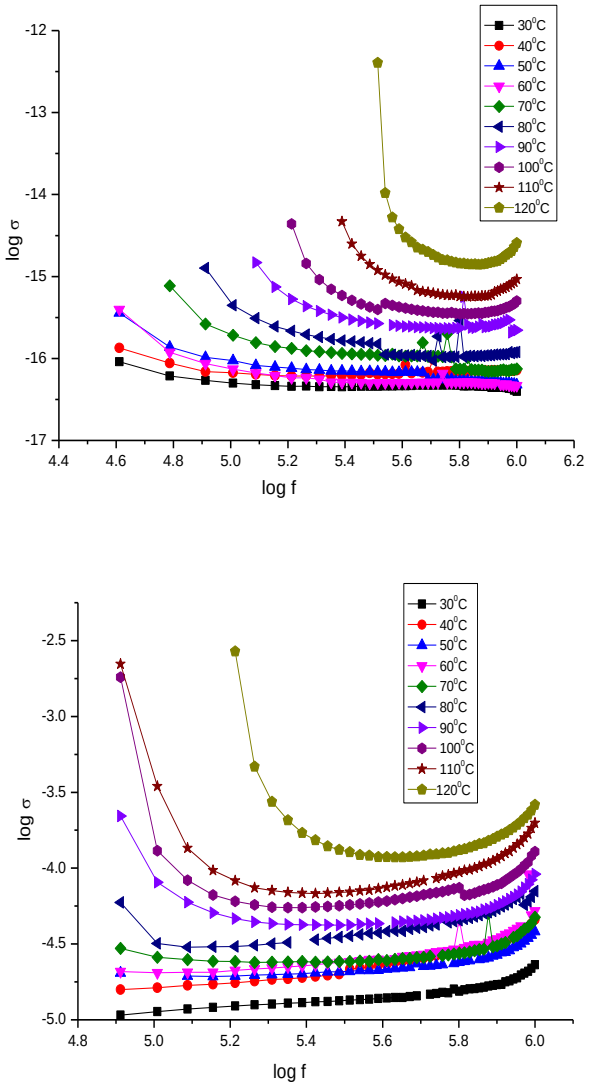

Figure 3:- (a-c): Variation of log σ with frequency for $LiNi_{1/3}Co_{0.28333}Zn_{0.05}Mn_{1/3}O_2$, $LiNi_{1/3}Co_{0.23333}Zn_{0.1}Mn_{1/3}O_2$ and $LiNi_{1/3}Co_{0.18333}Zn_{0.15}Mn_{1/3}O_2$.

Figures 4(a-c) show the variation of AC conductivity as a function of temperatures for some selected frequencies for $LiNi_{1/3}Co_{(1/3-X)}Mn_{1/3}Zn_XO_2$ (x= 0.05, 0.1and 0.15). From the slope of the graph, activation energies are calculated to be in the range from 0.34 to 0.8 eV. It is also found that the increase in conductivity with increasing temperature indicates a characteristic activated behaviour for the temperature range studied as indicated in table 2. The analysis of the frequency-dependent conductivity suggests that the electrical conduction in $LiNi_{1/3}Co_{(1/3-X)}Mn_{1/3}Zn_XO_2$ (x= 0.05, 0.1 and 0.15) is presumably caused by the hopping of lithium-ions between octahedral sites of the layered framework.

Table 2:- AC conductivity values for $LiNi_{1/3}Co_{0.28333}Zn_{0.05}Mn_{1/3}O_2$, $LiNi_{1/3}Co_{0.23333}Zn_{0.1}Mn_{1/3}O_2$ and $LiNi_{1/3}Co_{0.18333}Zn_{0.15}Mn_{1/3}O_2$

Temperature (°C)	AC conductivity (S/cm)		
	$LiNi_{1/3}Co_{0.28333}Zn_{0.05}Mn_{1/3}O_2$	$LiNi_{1/3}Co_{0.23333}Zn_{0.1}Mn_{1/3}O_2$	$LiNi_{1/3}Co_{0.18333}Zn_{0.15}Mn_{1/3}O_2$
40	5.71×10^{-7}	4.1×10^{-7}	3×10^{-7}
50	1.05×10^{-6}	1.3×10^{-6}	7.16×10^{-7}
60	9×10^{-6}	2.1×10^{-6}	4.6×10^{-6}
70	8×10^{-6}	2.7×10^{-6}	4.7×10^{-6}
80	7.3×10^{-6}	5×10^{-6}	5.46×10^{-6}
90	$\times 10^{-6}$	1.3×10^{-5}	1.19×10^{-5}
100	6.8×10^{-6}	1.7×10^{-5}	2.21×10^{-5}
110	1.2×10^{-5}	1.4×10^{-5}	5.02×10^{-5}
120	2.74×10^{-5}	3.5×10^{-5}	7.56×10^{-5}

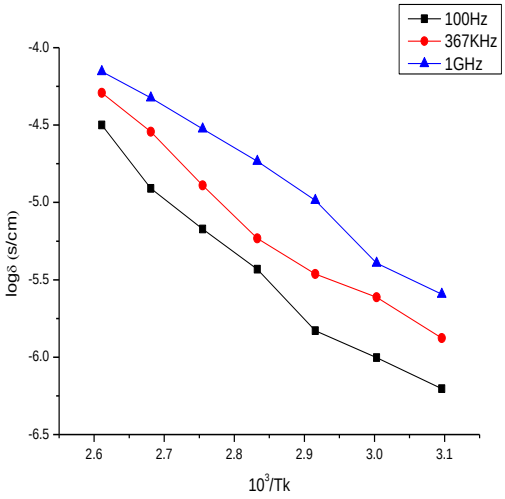

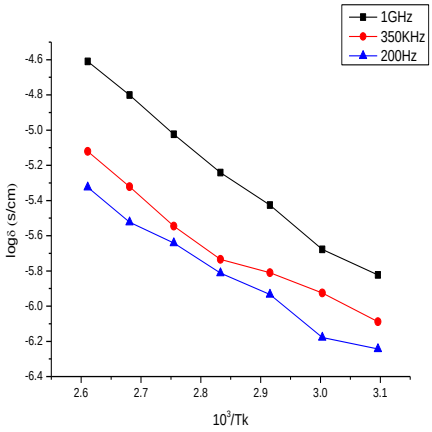

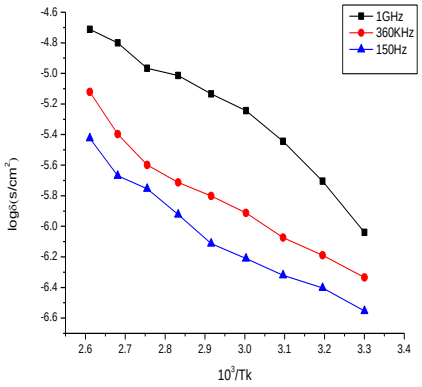

Figure 4:- (a-c) Arrhenius plots of AC conductivity for $LiNi_{1/3}Co_{0.28333}Zn_{0.05}Mn_{1/3}O_2$, $LiNi_{1/3}Co_{0.23333}Zn_{0.1}Mn_{1/3}O_2$ and $LiNi_{1/3}Co_{0.18333}Zn_{0.15}Mn_{1/3}O_2$

Variation of Impedance with Frequency:-

Figures 5(a-c) and 6(a-c) show the variation of real and imaginary impedance (Z' and Z") with frequency at different temperatures for the cathode $LiNi_{1/3}Co_{(1/3-X)}Mn_{1/3}Zn_XO_2$ (x= 0.05, 0.1 and 0.15) materials. The Z' value is found to decrease with increasing frequency at all temperatures. The Z" also decreased with increasing temperature, which is due to an increase in the conducting losses. The graph is composed of a semicircular area at high frequency and a curve at low frequency. The semicircle is probably due to resistance of the active material inside and on the interfaces of the electrodes, and the curve is due to diffused resistance of Li-ions in the electrolyte [25]. The frequency corresponding to Z''_{max} shifted to higher values with increasing temperature. The peak heights for both the peaks are decreased with increase of temperature indicating an increase in the conducting loss. The conductivity relaxation mechanism is temperature independent and slight deviation in higher temperature may be due to the ionic transport in materials is affected by structural aspects. Layered structured cathode materials had constant ionic concentration, but at higher temperature, the volume of the unit cell is increasing with temperature.

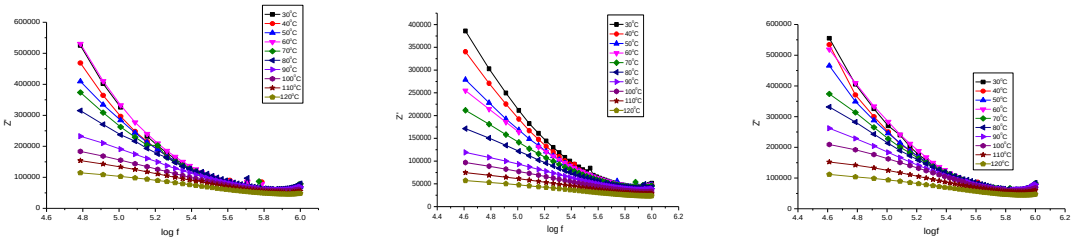

Figure 5:- (a-c) :Variation of real part of impedance (Z') with frequency for $LiNi_{1/3}Co_{0.28333}Zn_{0.05}Mn_{1/3}O_2$, $LiNi_{1/3}Co_{0.23333}Zn_{0.1}Mn_{1/3}O_2$ and $LiNi_{1/3}Co_{0.18333}Zn_{0.15}Mn_{1/3}O_2$.

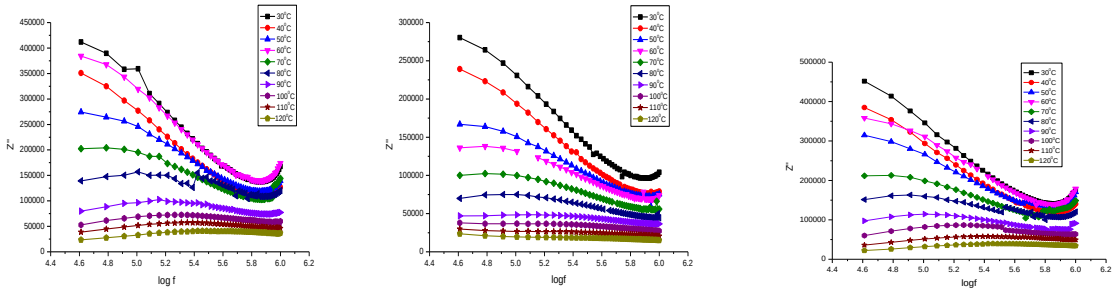

Figure 6:- (a-c) :Variation of imaginary part of impedance (Z') with frequency for $LiNi_{1/3}Co_{0.28333}Zn_{0.05}Mn_{1/3}O_2$, $LiNi_{1/3}Co_{0.23333}Zn_{0.1}Mn_{1/3}O_2$ and $LiNi_{1/3}Co_{0.18333}Zn_{0.15}Mn_{1/3}O_2$.

Electrical permittivity:

Fig.7 (a-c) shows the frequency dependence of the dielectric constant (ε') at different temperatures for $LiNi_{1/3}Co_{(1/3-x)}Mn_{1/3}Zn_xO_2$ (x= 0.05, 0.1and 0.15). It is observed that ε' gradually decreases with increasing frequency in a given temperature range. On increasing temperature, ε' increases apparently, which becomes even more significant at low frequency. The decrease in ε' is due to the space charges, which leads to the high dielectric constant and significant frequency dispersion [26, 27]. This indicates the thermally activated nature of the dielectric relaxation of the system [28]. From the frequency dependent plot of ε', it is observed that the value of ε' decreases sharply as the frequency increases and attains a constant limiting value, at which ε' becomes almost frequency independent. The higher values of dielectric constant at low frequencies can be due to pile-up of charges at the interfaces between the sample and the electrode. This can be explained based on the behaviour of the dipole movement as follows. Dielectric behaviour of samples with frequency is related to the applied electric field. An alternating electric field changes its direction with time. With each direction reversal, the polarization components are required to follow the field reversal. So, the polarization depends on the ability of dipoles to orient themselves in the direction of the field during each alternative change of the field. At low frequency regions the dipoles will get sufficient time to orient themselves completely along the direction of the field, resulting in larger values of ε' of the samples [29]. As the frequency increases further, the dipoles in the sample cannot reorient themselves fast enough to respond to the applied electric field, resulting in the decrease in ε' of the samples and becoming almost constant [30-31].

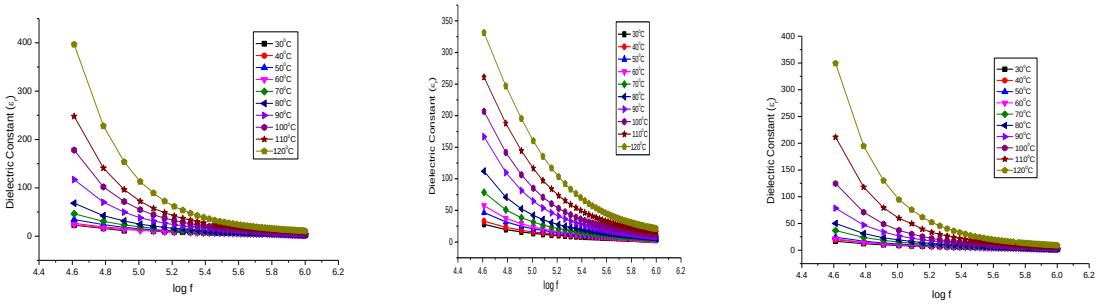

Figure 7:- (a-d): Frequency dependence of the dielectric constant (ε_r) for $LiNi_{1/3}Co_{0.28333}Zn_{0.05}Mn_{1/3}O_2$, $LiNi_{1/3}Co_{0.23333}Zn_{0.1}Mn_{1/3}O_2$ and $LiNi_{1/3}Co_{0.18333}Zn_{0.15}Mn_{1/3}O_2$.

Conclusion:-

The Zinc substituted layered $LiNi_{1/3}Co_{(1/3-X)}Mn_{1/3}Zn_xO_2$ ($0.05 \leq x \leq 0.2$) cathode materials are successfully synthesized by high temperature solid-state reaction method. Different properties of the materials are studied using different techniques. The X-ray diffraction (XRD) patterns possessed the layered structure of the hexagonal α-$NaFeO_2$ structure with a space group of $R\bar{3}m$. An AC impedance spectroscopic technique was used to correlate between the microstructure and electrical properties of the compound. The presence of grain bulk effect in the compound was observed. The frequency-dependent electrical data were used to study the conductivity mechanism. An analysis of the electric impedance with frequency at different temperatures has provided some information to support suggested conduction mechanism.

References:-

1. Liu, Z., A. Yu, and J.Y. Lee (1999): Synthesis and characterization of $LiNi_{1-x-y}Co_xMn_yO_2$ as the cathode materials of secondary lithium batteries. J. Power Sources, 81-82: 416-419.
2. Yoshio, M., Hideyuki N., Jun-ichi Itoh, Masaki Okada, Takashi Mouri, (2000): Preparation and properties of $LiCo_yMn_xNi_{1-x-y}O_2$ as a cathode for lithium ion batteries. J. Power Sources. 90: 176-181.
3. Ohzuku, T., Makimura, Y., (2001): Layered lithium insertion material of $LiNi_{1/3}Co_{1/3}Mn_{1/3}O_2$ for lithium ion batteries J. Chem. Lett., 7: 642-643.
4. Hwang, B. J., Tsai, Y.W., Carlier, D., Ceder, G. (2003): A Combined Computational / Experimental Study on $LiNi_{1/3}Co_{1/3}Mn_{1/3}O_2$ Chem. Mater. 15: 3676-3682.
5. Shaju, K. M., Rao, G. V. S., Chowdari, B. V. R. (2002): Performance of layered $LiNi_{1/3}Co_{1/3}Mn_{1/3}O_2$ as cathode for Li-ion batteries. Electrochim. Acta, 48: 145-151.
6. Reddy, M. V., Rao, G. V. S., Chowdari, B. V. R. (2006): Synthesis by molten salt and cathodic properties of $Li(Ni_{1/3}Mn_{1/3}Co_{1/3})O_2$, J. Power Sources, 159: 263- 267.

7. Yabuuchi, N., Ohzuku, T. J. (2003): Novel lithium insertion material of $LiNi_{1/3}Mn_{1/3}Co_{1/3}O_2$ for advanced lithium ion batteries, J. Power Sources, 119-121: 171-174.
8. Chebiam, R. V., Prado, F., Manthiram, A. (2001): Soft Chemistry Synthesis and Characterization of Layered $Li_{1-x}Ni_{1-y}Co_yO_{2-\delta}$ ($0 \leq x \leq 1$ and $0 \leq y \leq 1$) Chem. Mater. 13: 2951-2957.
9. Kim, H. S., Kong, M., Kim, K., Kim, I. J., Gu, H. B. (2007): Effect of carbon coating on $LiNi_{1/3}Co_{1/3}Mn_{1/3}O_2$ cathode material for lithium secondary batteries. J. Power Sources, 171: 917-921.
10. Na, S. H., Kim, H. S., Moon, S. I. (2005): The effect of Si doping on the electrochemical characteristics of $LiNi_xMn_yCo((_{1-x-y}))O_2$, Solid State Ionics, 176: 313-317.
11. Sun, Y. K., Lee, Y. S., Yoshio, M., Amine, K. (2002): Synthesis and Electrochemical Properties of ZnO-Coated $LiNi_{0.5}Mn_{1.5}O_4$ Spinel as 5 V Cathode materials for lithium secondary batteries electrochem. solid-state lett. 5(5): A99-A102.
12. Koyama, Y., Tanaka, I., Adachi, H., Makimura, Y., Ohzuku, T. (2003): Crystal and electronic structures of super structural $Li_{1-x}Ni_{1/3}Mn_{1/3}Co_{1/3}O_2$, J. Power Sources, 119-121: 644-648.
13. Chen, Y.H., Chen, R.Z., Tang, Z.Y., (2009): Synthesis and characterization of Zn doped $LiCo_{0.3}Ni_{0.4-x}Mn_{0.3}Zn_xO_2$ cathode materials for lithium ion batteries, J. Alloys Compds, 476: 539-542.
14. Ren, H. B., Li, X., Peng, Z. H. (2011): Electrochemical properties of $Li[Ni_{1/3}Mn_{1/3}Al_{1/3-x}Co_x]O_2$ as a cathode material for lithium ion battery, Electrochim. Acta, 56: 7088-7091.
15. Milewska, A., Molenda, M., Mokenda, (2011): Structural, transport and electrochemical properties of $LiNi_{1-y}Co_yMn_{0.1}O_2$ and Al,Mg and Cu-substituted $LiNi_{0.65}Co_{0.25}Mn_{0.1}O_2$ oxides, J. Solid State Ionics 192: 313-320.
16. B. J. Hwang, Y. W. Tsai, D. Carlier, and G. Ceder, (2003): A combined computational/experimental study on $LiNi_{1/3}Co_{1/3}Mn1_{/3}O_2$, Chemistry of Materials, 15: 3676-3682.
17. L. A. Riley, S. Van Atta, A. S. Cavanagh, (2011): Electrochemical effects of ALD surface modification on combustion synthesized $LiNi_{1/3}Co_{1/3}Mn1_{/3}O_2$ as a layered-cathode material, J. Power Sources, 196: 3317-3324.
18. C.T. Hsieh, C.Y. Mo, Y.F. Chen, and Y.J. Chung, (2013): Chemical wet synthesis and electrochemistry of $LiNi_{1/3}Co_{1/3}Mn1_{/3}O_2$cathode materials for Li-ion batteries, Electrochim. Acta, 106: 525-533.
19. Kyung K. L. (2000): Electrochemical and structure characterization in $LiNi_{1-y}Co_yO_2(0 \leq y \leq 0.2)$ position electrodes during initial cycling. J Electrochem Soc, 147: 1715-1723.
20. R. Koksbang, I. I. Olsen, P. E. Tonder, N. Knudsen, D. Fauteux, (1991): Polymer electrolyte lithium batteries rechargeability and positive electrode degradation: An AC impedance study, Electrochem. 21: 301-307.
21. P. Periasamy, N. Kalaiselvi, H.S. Kim, (2007): High voltage and high capacity characteristics of $LiNi_{1/3}Co_{1/3}Mn_{1/3}O_2$ cathode for lithium battery applications, Int. J. Electrochem. Sci., 2: 689-699.
22. G. Montesperelli, P. Nunziante, M. Pasquili, G. Pistoia, (1990): Li passivation in different electrolytes during storage and cycling - An impedance spectroscopy study, Solid State Ionics 37: 149-156.
23. M. Gaberscek, S. Pejovnik, (1996): Impedance spectroscopy as a technique for studying the spontaneous passivation of metals in electrolytes, Electrochim. Acta 41: 1137-1142.
24. F.Capuano,F.Croce, B.Scrosati, (1991): Composite Polymer Electrolytes, J. Electrochem. Soc., 138 1918-1922.
25. M. Saiful Islam and Craig A. J. Fisher, (2014): Lithium and sodium battery cathode materials: computational insights into voltage, diffusion and nanostructural properties, Chem. Soc. Rev. 43: 185-204.
26. Gerhardt R. (1994): Impedance and dielectric spectroscopy revisited: distinguishing localized relaxation from long-range conductivity, J. Phys. Chem. Solids, 55: 1491-1506.
27. O. Bohnke, J. Emery, J.K. Fourquet, (2003): Anomalies in Li+ ion dynamics observed by impedance spectroscopy and Li NMR in the perovskite fast ion conductor Solid State Ionics, 158: 119-132.
28. B. Ellis, P.S. Herle, Y.H. Rho, L.F. Nazar, R. Dunlap, L.K. Perry, D.H. Ryan, (2007): Nanostructured materials for lithium-ion batteries: Surface conductivity vs. bulk ion/electron transport Faraday Discussions, 134: 119-141.
29. K. Rissouli, K. Benkhouja, J.R. Ramos-Barrado, C. Julien, (2003): Electrical conductivity in lithium orthophosphates Materials Science and Engineering B, 98: 185-189.
30. K. Funke, (1993): Prog. Jump relaxation in solid electrolytes Solid State Chem. 22: 111-195.
31. K. Anand, B. Ramamurthy, V. Veeraiah, K. Vijaya Babu, (2016): Structural, dielectric and conductivity studies of $LiNi_{0.75}Mg_{0.25-x}Cu_xPO_4$ synthesized by solid state reaction method, Processing and Application of Ceramics, 10: 47-55.